Characterisation of a mitochondrial iron transporter of the pathogen *Trypanosoma brucei*

Fuli Zheng[1,3#], Claudia Colasante[2#], Frank Voncken[3*]

[1]Department of Preventive Medicine, School of Public Health, Fujian Medical University, Xueyuan Road, Fujian, 350122, P.R. China

[2]Institute for Anatomy and Cell Biology, Division of Medical Cell Biology, Aulweg 123, University of Giessen, 35392 Giessen, Germany

[3]Department of Biomedical Sciences, School of Life Sciences, University of Hull, Cottingham Road, Hull, HU6 7RX, United Kingdom

[#] These authors contributed equally to the paper

Running Title: The *T. brucei* mitochondrial iron transporter *Tb*MCP17

*To whom correspondence should be addressed: Claudia.Colasante@anatomie.med.uni-giessen.de

Keywords: mitochondrial transport, iron metabolism, *Trypanosoma brucei*, mitochondrial carrier family-proteins

ABSTRACT

Similar to higher eukaryotes, the protist parasite *T. brucei* harbours several iron-containing proteins that regulate DNA and protein processing, oxidative stress defence and mitochondrial respiration. The synthesis of these proteins occurs either in the cytoplasm or within the mitochondrion. For mitochondrial iron cluster protein synthesis iron needs to be transported across the solute impermeable mitochondrial membrane. In *T. brucei* we previously identified 24 mitochondrial carrier proteins (*Tb*MCPs) sharing conserved structural and functional features with those from higher eukaryotes. One of these carriers (*Tb*MCP17) displayed high similarity with the iron carriers MRS3, MRS4 from yeast and mitoferrin from mammals, insects and plants. In the present study we demonstrated that *Tb*MCP17 functions as an iron carrier by complementation studies using MRS3/4-deficient yeast. Depletion of *Tb*MCP17 in procyclic form *T. brucei* resulted in growth deficiency, increased sensitivity to iron deprivation, and lowered mitochondrial iron content. Taken together our results suggest that *Tb*MCP17 functions as a mitochondrial iron transporter in the parasite *T. brucei*.

34 **INTRODUCTION**

35 *Trypanosoma brucei* is a protist parasite belonging to the class of the Kinetoplastida and
36 causing African sleeping sickness in humans and Nagana in cattle [1–3]. During its life cycle,
37 the parasite is transferred from the insect vector, the tsetse fly, to the mammalian host thereby
38 undergoing substantial remodelling in morphology and metabolism [4]. *T. brucei* replicative
39 stages that can be cultured *in vitro* are the bloodstream form (BSF) found in the blood and
40 cerebrospinal fluid of mammals, and the procyclic form (PCF) residing in the mid-gut of the
41 tsetse fly. The BSF, which lives in a glucose rich environment, derives its energy exclusively
42 through substrate level phosphorylation reactions during glycolysis that is partially located
43 within specialised peroxisomes (glycosomes) [5,6]. Within the insect vector, PCF *T. brucei*
44 uses glucose and the amino acid proline to generate ATP through glycolysis and mitochondrial
45 respiration [5,7–11].

46 As the energy metabolism, the mechanism by which iron and heme are taken up is adapted to
47 iron availability within the hosts and differs between BSF and PCF. The BSF acquires
48 transferrin-bound iron and heme in the form of a haptoglobin–haemoglobin complex through
49 receptor mediated endocytosis directed to the endo-lysosomal system [12–15]. Due to the
50 absence of transferrin in the insect gut, the PCF takes up ferrous iron by endocytosis of reduced
51 ferric complexes [16] while heme is acquired through the membrane transporter *Tb*Hrg [15].
52 Once within the cytoplasm, iron and heme are redistributed to intracellular sites for the
53 synthesis of iron-containing protein. Like higher eukaryotes, *T. brucei* incorporates iron into
54 iron/sulphur clusters (Fe/S) or as non-heme and non-Fe/S iron into enzymes involved in
55 cellular processes such as DNA synthesis, protein translation, oxidative stress defence and
56 cytochrome respiration [12,14,17]. Iron-dependent enzymes that have been identified in *T.*
57 *brucei* are, for example, the ribonucleotide reductase that catalyses the reduction of
58 ribonucleotides to deoxyribonucleotides necessary for DNA synthesis [18,19], superoxide

59 dismutase, which catalyses the dismutation of the superoxide radical ($O_2^{\cdot -}$) into hydrogen
60 peroxide [20], alternative oxidase, which re-oxidises glycolysis derived NADH [21–23],
61 aconitase and fumarase, both TCA cycle enzymes [24] or the cytochromes of the respiratory
62 chain [25]. Machineries responsible for the mitochondrial and cytosolic iron–sulphur cluster
63 protein assembly and for the mitochondrial transfer of iron to non-heme/non-FeS iron proteins
64 have all been identified in *T. brucei* [12,26]. The mitochondrion is an indispensable site for
65 the synthesis of iron-sulphur cluster proteins involved in electron transport during respiration,
66 enzymatic catalysis, oxidative stress response and the regulation of mitochondrial iron
67 homoeostasis [27]. For the assembly of these iron-containing proteins, iron has to cross the
68 solute-impermeable inner mitochondrial membrane. In yeast and vertebrates iron is imported
69 into the mitochondrion by the mitochondrial iron transporters MRS3 and 4 [28–30], and
70 mitoferrin, respectively [31]. These transporters all belong to the mitochondrial carrier family
71 (MCF, SLC25A), which exchange various solutes, including carboxylates, nucleotides,
72 inorganic phosphate ornithine, carnitine, and glutamine across the mitochondrial inner
73 membrane [32,33]. MCF proteins (MCPs) control the influx rate of metabolic intermediates
74 into the mitochondrion, regulate the flux through metabolic processes and maintain the cellular
75 redox and ATP homeostasis [34]. The protein structure of MCPs is conserved and consist of
76 six transmembrane domains connected by short hydrophilic loops. Each odd numbered
77 transmembrane domain and hydrophilic loop contains a conserved signature motif [33] and
78 amino acid contact points, which determine the substrate specificity of the carrier subtype [35].
79 We previously reported that *T. brucei* possesses 24 MCPs (*Tb*MCPs) containing conserved
80 structural and sequence features of MCPs from higher eukaryotes [36–39]. Amongst these
81 carriers we identified one with high similarity to MRS3, MRS4 and mitoferrin and named it
82 *Tb*MCP17 [36]. In the present study, sequence alignments and phylogenetic reconstruction
83 revealed the close relationship of *Tb*MCP17 to plant and mammalian iron carriers. The

84 functionality of *Tb*MCP17 as an iron carrier was confirmed by complementation studies using
85 MRS3/4-deficient yeast. We also show that in PCF, the removal of *Tb*MCP17 caused a
86 significant growth defect, increased the sensitivity to iron deprivation, and lowered the
87 mitochondrial iron content. Taken together, our findings suggest that *Tb*MCP17 functions as
88 a mitochondrial iron transporter in the parasite *T. brucei*.
89
90

91 **MATERIALS AND METHODS**

92

93 **Phylogenetic reconstruction and sequence analysis**

94 Multiple sequence alignments were generated using ClustalO [40,41]. Phylogenetic trees were
95 constructed using MEGA7 (Molecular Evolutionary Genetics Analysis version 7.0; [42].
96 Protein-Blast (blast.ncbi.nlm.nih.gov) was used to retrieve iron carrier protein sequences from
97 trypanosomatids, plants, insects, fungi and mammals. These were then imported into MEGA7
98 and aligned. Using the neighbour-joining (NJ) method [43], a NJ tree was drawn with bootstrap
99 set to 1000.

100 The GenBank (gb), EMBL (emb), NCBI (XP) and Swiss protein (sp) accession numbers for
101 the *Tb*MCP17 alignment and the phylogenetic reconstruction were as follows: *Tb*MCP17,
102 *Trypanosoma brucei brucei* Tb927.3.2980; *Trypanosoma brucei gambiense*
103 emb_CBH09968.1; *Trypanosoma congolense* emb_CCC89759.1; *Trypanosoma vivax*
104 emb_CCC47046.1; *Trypanosoma cruzi* XP_822091.1; *Trypanosoma vivax* gb_EKG04497.1;
105 *Trypanosoma rangeli* gb_ESL10208.1; *Leishmania amazonensis* gb_ALP75642.1;
106 *Leishmania mexicana* emb_CBZ23750.1; *Leishmania major* emb_CBZ12619.1; *Leptomonas*
107 *seymouri* gb_KPI87731.1; *Leishmania panamensis* gb_AIO00226.1; *Ustilago hordei*
108 emb_CCF54811.1; *Ustilago maydis* gb_KIS71149.1; *Pseudozyma brasiliensis*
109 gb_EST06361.1; *Rhizopus microspores* emb_CEJ04189.1; *Moesziomyces antarcticus*
110 gb_ETS61106.1; *Drosophila willistoni* gb_EDW83029.1; *Bactrocera cucurbitae*
111 XP_011180944.1; *Drosophila mojavensis* gb_EDW14539.1; *Gossypium raimondii*
112 gb_KJB83905.1; *Fragaria vesca* XP_004294768.1; *Madurella mycetomatis* gb_KOP45184.1;
113 *Phanerochaete carnosa* gb_EKM49983.1; *Gossypium arboreum* gb_KHG15442.1;
114 *Rhizoctonia solani* emb_CUA78164.1; *Drosophila virilis* gb_EDW59237.2; *Botrytis cinerea*
115 XP_001553628.1; *Sesamum indicum* XP_011080718.1; *Homo sapiens* (MFRN1)

116 gb_EAW63617.1; *Homo sapiens* (MFRN2) gb_AAK49519.1; *Saccharomyces cerevisiae*
117 (MRS3p), gb_EGA61827.1; *Saccharomyces cerevisiae* (MRS4p) gb_AJS43107.1;
118 *Arabidopsis thaliana* gb_AAP42736.1; *Zea mays* (MRS3) gb_ACG42379.1; *Mus musculus*
119 (MFRN1) gb_AAL23859.1; *Mus musculus* (MFRN2) gb_AAH25908.1; *Bos taurus* (MFRN1)
120 gb_AAI03256.1; *Bos taurus* (MFRN2) NP_001192481.1; *Lucilia cuprina* gb_KNC31521.1;
121 *Drosophila busckii* gb_ALC47563.1; *Harpegnathos saltator* gb_EFN83637.1; *Acyrthosiphon*
122 *pisum* NP_001280444.1; *Aspergillus niger* XP_001390994.2.
123
124 **Culture and transfection of *Trypanosoma brucei***
125 Procyclic form PCF449 were grown in a 27 °C incubator in MEM-PROS medium [24]
126 supplemented with 10% heat-inactivated foetal bovine serum (Lonza), 2.5 mg/ml of heme (in
127 100 mM NaOH) 1% of penicillin/streptomycin solution (Sigma) and 5 mM proline (Sigma).
128 For the experiments described in this paper *Trypanosoma brucei* cell lines were transfected
129 with different plasmids and clonal cell lines were selected using antibiotics according to the
130 previously published protocol [44].
131
132 **Yeast functional complementation**
133 *Saccharomyces cerevisiae* strains used in this study were wildtype strain BY4741 (MATa
134 his3Δ1 leu2Δ0 met15Δ0 ura3Δ0, referred to as wild type below) and mitochondrial iron carrier
135 (MRS3/4) deficient strain GW403 (mrs3/4Δ; MATa his3-Δ1 leu2-3 leu2-112 ura3-52 trp1-
136 289 mrs3Δ::loxP mrs4Δ::loxP; referred to as ΔMRS3/4 below) [45]. Yeast strains were
137 maintained on standard YPD medium. For clone-selection following transfection, synthetic
138 complete (SC) medium without uracil (0.67% yeast nitrogen base without amino acids, 1.4%
139 drop-out medium supplements without histidine, leucine, tryptophan and uracil) supplemented
140 with 60 mg/L of leucine, 20 mg/L of tryptophan, 20 mg/L of histidine, 2% of agar and 2% of

141 dextrose was used. To test cell growth on different carbon sources, YPD and YPG media were
142 used. For plate growth experiments, SC medium was supplemented with dextrose (SCD
143 medium) or glycerol (SCG medium). To simulate iron deprived condition, 80 μM of iron
144 chelator bathophenanthrolinedisulfonic acid (BPS, Sigma) was added to the SC medium.
145 The complete open reading frames of *Tb*MCP17 and *S. cerevisiae* MRS3 (YJL133W) were
146 PCR-amplified using the primer combination 5'-gaGGATCCatggtttccgagggcacttccgctg-3'/5'-
147 cgAAGCTTttaccgttcctccatgaacttcttggc-3', and 5'-gaGGATCCatggtagaaaactcgtcgagtaata-
148 3'/5'-cgCTGCAGctaatacgtcattaggaaatgttttgcacattc -3', respectively. Restriction enzyme sites
149 used for subsequent cloning into the yeast centromeric expression vector pCM190 (Euroscarf)
150 are underlined and capitalised.
151 Plasmids containing either *Tb*MCP17 or MRS3 were transformed into the yeast strain GW403,
152 using the lithium acetate/single-stranded carrier DNA method described by Gietz and Woods
153 [46]. Obtained yeast clones were maintained on synthetic complete dextrose (glucose) medium
154 without uracil in the presence of tetracycline. Heterologous protein expression in yeast was
155 induced by tetracycline removal [47].
156 For the growth experiments, yeast cells from an overnight starter culture were inoculated in
157 20 ml of medium and the OD_{600} measured every 3 to 4 h until cells reached stationary phase.
158 For plating experiment, yeast was spotted on agar plates at OD_{600} 1, 0.1, 0.01 and 0.001.
159

160 **Over-expression of *Tb*MCP17**

161 The open reading frame (ORF) of *TbMCP17* was amplified from *T. brucei* 449 genomic DNA
162 using the primer pair 5'-ggacggAAGCTTaccatggtttccgagggcacttccgctg-3'/5'-
163 gcttgcaGGATCCccgttcctccatgaacttcttggc-3'. The restriction sites used for subsequent cloning
164 into the pHU1 or pHU2 *T. brucei* expression vectors [48] are underlined and capitalised. The
165 expression vectors generate either C-terminally (pHU1) or N-terminally (pHU2) 2×myc-

166 tagged recombinant proteins. Comparison of the cloned *TbMCP17* sequence with the sequence
167 obtained from the genome sequence database (GeneDB) of *T. brucei* strain 927 revealed only
168 a few sequence differences at the DNA level, but none in the predicted amino acid sequence.
169 The obtained vectors were used to transfect the PCF *Trypanosoma brucei* strain Lister 427,
170 stably expressing the tetracycline (tet) repressor from the plasmid pHD449 (PCF449).
171 Hygromycin resistant clonal cell lines were isolated and analysed by western blotting after
172 induction of tagged *Tb*MCP17 expression using tetracycline (0.5 mg/ml). The generated cell
173 lines are further referred to as *Tb*MCP17-cmyc^{ti} (C-terminally-tagged *Tb*MCP17) and
174 *Tb*MCP17-nmyc^{ti} (N-terminally-tagged *Tb*MCP17).
175
176 **Immunofluorescence analysis**
177 Immunofluorescence analysis using paraformaldehyde-fixed trypanosomes was performed as
178 previously described [36] with minor adjustments: an aliquot of culture containing
179 approximately 1×10^7 cells was stained with 0.5 µM Mitotracker Red CMXRos (Sigma) for 30
180 min. Cells were then fixed onto coverslips using freshly made 4% (w/v) paraformaldehyde in
181 1x PBS and left to attach overnight at 4°C. For permeabilisation 0.2% (w/v) Triton X-100 was
182 added followed by incubation with 0.5% (w/v) gelatine in 1x PBS. Afterwards, myc-primary
183 antibody (Roche) was added to the coverslips at a dilution of 1:500 in 0.5% (w/v) gelatine in
184 1x PBS and incubated for 60 min. Coverslips were then washed twice in 1x PBS. A 1:500
185 dilution of the secondary antibody in 0.5% (w/v) gelatine in 1x PBS (Alexa Fluor 488 goat
186 anti-mouse, Thermofisher) was then added and incubated for 60 min in the dark. The coverslip
187 was placed on a microscope slide coated with mounting medium containing DAPI (Thermo).
188 Slides were stored in the dark at 4°C and analysed using a laser scanning confocal microscope
189 (Zeiss) within 2-3 days.
190

191 **Generation of the conditional *Tb*MCP17 double-knock out cell line**

192 The conditional double knock out of *TbMCP17* was constructed using the target gene
193 replacement method [39,49,50]. The cell line *Tb*MCP17-cmyc^{ti} was used as parental cell line
194 for the generation of the conditional *TbMCP17* double-knock out cell line. The 5'-UTR and
195 3'-UTR of *TbMCP17* were PCR amplified using the primer pairs 5'-
196 gctaGAGCTCcgtgtcgtgaggtggagaggtgatg-3'/5'-
197 gctaACTAGTcacacatcaccgcagccaagcaaaacaacg-3' (5'-UTR 475 bp fragment), and 5'-
198 gcatGGATCCccgtgttcttgtttcaggtgtgaacc-3'/5'-ctatGGGCCCgtcaaacacattactggagcgg-3' for
199 the (3'-UTR 484 bp fragment). Using the underlined and capitalised restriction enzyme sites
200 the amplified fragments were inserted on either side of the NEO (G418) (NEO-*TbMCP17*-
201 knock out vector) and BSD (blasticidin) (BSD-*TbMCP17*-knock out vector) antibiotic
202 resistance cassettes, bearing actin 5'-splice sites and actin 3'-UTR [50]. After transfection of
203 the *Tb*MCP17-cmyc^{ti} cell line with the NEO-*TbMCP17*-knock out construct and clonal
204 selection with 15 µg/ml G418, the single-knock out cell line
205 Δ*TbMCP17*::NEO/*TbMCP17*/*TbMCP17*-cmyc^{ti} was obtained. The double knock out cell line
206 Δ*TbMCP17*::NEO/Δ*TbMCP17*::BSD/*TbMCP17*-cmyc^{ti}, (further referred to as
207 Δ*TbMCP17*/*TbMCP17*-cmyc^{ti} in this paper), was obtained after transfection of the
208 Δ*TbMCP17*::NEO/*TbMCP17*/*TbMCP17*-cmyc^{ti} cell line using the BSD-*TbMCP17*-knock out
209 plasmid and clonal selection with 15 µg/ml G418 and 10 µg/ml blasticidin. The *TbMCP17*
210 single- and double-knock out cell lines were cultured in the presence of tetracycline (1 µg/ml)
211 to maintain *Tb*MCP17-cmyc expression and ensure cell viability. The deletion of *TbMCP17*
212 was confirmed by PCR analysis.

213

214 **Depletion of *TbMCP17* by RNA interference**

215 Inhibition of *TbMCP17* expression was performed in PCF *T. brucei* using RNA interference
216 (RNAi) [51]. The primer combinations 5'-gAAGCTTccaccccatttgatgttatcaagcagc-3'/5'-
217 ggCTCGAGtgactaagacatagcgcaccgcatcgg-3' and 5'-cGGATCCccatttgatgttatcaagcagcggatg-
218 3'/5'-cAAGCTTtccCTCGAGcattgacagggcaccagcaggagcg-3' were used to PCR amplify the
219 387 bp sense and 467 bp antisense sequences of *TbMCP17,* respectively. The restriction
220 enzyme sites used for subsequent cloning into the vector pHD676 are underlined and
221 capitalised. The pHD676-*TbMCP17* RNAi vector was used for transfection of procyclic form
222 *T. brucei* PCF449. The *Tb*MCP17RNAi cell line was obtained after clonal selection using
223 hygromycin (25 µg/ml) and phleomycin (0.5 µg/ml).
224
225 **PCF *T. brucei* growth analysis**
226 For growth analysis, PCF cultures were diluted to a density of 5×10^5 cells/ml at the start of the
227 experiments. During the growth experiments of the *Tb*MCP17 overexpressing cells
228 (*Tb*MCP17-cmyc^{ti} and *Tb*MCP17-nmyc^{ti}), 10 µg/ml tetracycline were added daily to maintain
229 expression of the recombinant myc-tagged proteins. During the growth experiments of cells
230 depleted of *Tb*MCP17 by conditional knock out (Δ*TbMCP17*/*TbMCP17*-cmyc^{ti}) tetracycline
231 was removed from the cell culture 24 h prior the start of the growth experiments and cells were
232 thoroughly washed using MEM-Pros to stop the expression of *Tb*MCP17-cmyc. During the
233 growth experiments of cells in which *Tb*MCP17 was depleted by RNAi 10 µg/ml tetracycline
234 were added daily to induce and maintain the RNA interference. Cell densities were determined
235 every 24 h using a haemocytometer. In some experiments, the iron chelator deferoxamine
236 (Sigma) was added at different concentrations (10 µM to 100 µM) to obtain iron deprived
237 conditions.
238 **Western Blot**

239 For each SDS-PAGE lane 5×10^6 cells were pelleted, resuspended in denaturing SDS-
240 containing Laemmli buffer, and heated at 95°C for 5 min. Proteins were separated on a 12%
241 SDS-PAGE and then transferred to PVDF (GE Health Care Life Sciences) membranes at 100
242 V for 50 min in Towbin buffer (48 mM Tris, 39 mM Glycine, 20% (v/v) methanol, pH 8.3).
243 Membranes were blocked with 5% w/v skimmed milk in Tris-buffered saline buffer (TBS)
244 and 0.1% Tween-20 (milk/TBST) at room temperature for 1 h. Subsequently, membranes were
245 incubated with anti-c-myc (Roche) primary antibody diluted 1:2000 in milk/TBST, for 1 h at
246 room temperature. Membranes were then washed 3 times with excess TBST and incubated
247 with anti-mouse IgG HRP (Abcam) in secondary antibody diluted 1:2000 in milk/TBST, for
248 1 h at room temperature. Protein detection was performed using an ECL detection kit
249 (Amersham, GE Healthcare). Coomassie brilliant blue (CBB) staining was used as loading
250 control.
251
252 **Iron measurement**
253 Cells were grown in iron and heme depleted medium to avoid interference during iron
254 measurements. Depletion was achieved by pre-dialysing the foetal calf serum (FCS) using a
255 Slide-A-Lyzer™ G2 dialysis cassette, 2K molecular weight cut-off, 70 mL (Thermo)
256 according to manufacturer's protocol. Briefly, heat-inactivated FCS was added to the dialysis
257 cassette and put into 2 L of 1x PBS at 4°C for 3 h. After this time, the 1x PBS was discarded,
258 replaced by fresh 1x PBS and dialysis was repeated 2 times more. Medium was then prepared
259 using the dialysed FCS and without the addition of heme.
260 Mitochondria of *T. brucei* were isolated by digitonin-fractionation according to previously
261 published protocols [52]. Cellular and mitochondrial iron content were measured using a
262 colorimetric ferrozine-based assay [53] with some modifications. Briefly, 100 µl aliquots of
263 whole cell or mitochondrial lysates derived from 10^8 trypanosomes were placed in Eppendorf

264 tubes and mixed with 100 µl of 10 mM HCl, and 100 µl iron-releasing reagent (a freshly mixed
265 solution of equal volumes of 1.4 M HCl and 4.5% (w/v) $KMnO_4$). The mixture was then
266 incubated for 2 h at 60 °C within a fume hood. After cooling to room temperature, 30 µl of the
267 iron-detection reagent (6.5 mM ferrozine, 6.5 mM neocuproine, 2.5 M ammonium acetate, and
268 1 M ascorbic acid) were added to each tube. After 30 min, the absorbtion was measured at
269 550 nm. The iron content of the sample was calculated by comparing its absorbtion to that of
270 a range of equally treated iron ($FeCl_3$) standards (0–300 µM).
271
272 **qRT PCR**
273 One-step real time qPCR was used to determine the expression levels of *TbMCP17* after RNAi.
274 Total RNA was isolated from 1×10^7 PCF *T. brucei* using TriFast (PeqLab Biotechnology
275 GmbH) according to manufacturer´s protocol. For cDNA synthesis 2 µg total RNA in 10 µl
276 RNase-free water were mixed with 4 µl of 5× M-MuLV reaction buffer, 1 µl of RiboLock
277 RNase inhibitor, 2 µl of 10 mM dNTP, and 2 µl of M-MuLV reverse transcriptase (cDNA
278 synthesis kit, Thermo). The reaction was incubated at 25 °C for 5 min, followed by 60 min at
279 37 °C. Then the reaction was terminated by incubation at 70 °C for 5 min. RT-PCR for the
280 detection of *TbMPC17* was performed using 1 µl of synthesised cDNA and the QuantiTect
281 SYBR Green RT-PCR kit (QIAGEN) to set up a 25 µl PCR reaction. CT values of
282 experimental samples (in triplicates) were compared with wild type CT after normalising CT
283 from the house-keeping genes tubulin.
284
285 ***Tb*MCP17 antibody generation**
286 His-tagged *Tb*MCP17 was expressed in *E. coli* using the pET28a vector (Novagen). The
287 *Tb*MCP17 ORF was PCR amplified using the primers 5'-
288 ggacggAAGCTTaccatggtttccgagggcacttccgctg-3', 3'-

289 gcttgcaGGATCCccgttcctccatgaacttcttggc-5' and inserted into the vector using the restriction
290 enzyme sites *BamH* I and *Hind* III (underlined). The Lemo21(DE3) *E. coli* strain was used for
291 His-tagged *Tb*MCP17 expression. Transformed cells were inoculated in LB media with 50
292 µg/ml kanamycin and 30 µg/ml chloramphenicol and grown overnight. The next day the
293 overnight culture was diluted 1/50 and protein expression was started at OD_{600} 0.4-0.8 at 37
294 °C by the addition of 0.4 mM IPTG for 4 h.
295 Cells were harvested by centrifugation at 4,000×g for 10-20 min at 4 °C, resuspended in 5
296 ml/g pellet native resuspension buffer (50 mM Na-phosphate pH 8.0, 300 mM NaCl,
297 0.01%Tween-20) supplemented with protease inhibitor cocktail without EDTA (Sigma), 0.2
298 mg/ml lysozyme and 5 unit/µl DNase. After incubation on ice for 30 min cells were passed
299 through the French press until the lysate turned clear. *Tb*MCP17 inclusion bodies were pelleted
300 at 13,000×g for 30 min and solubilised using 5 M Urea or 1% sarcosyl. After solubilisation
301 *Tb*MCP17 was allowed to bind to 1 ml of Ni-NTA agarose (Qiagen)/20 ml of solubilised
302 protein, and the mixture was stirred for 60 min at room temperature. The Ni-NTA agarose was
303 washed according to the manufacturer´s protocol and *Tb*MCP17 was eluted using 200 µl
304 elution buffer (8 mM Na_2HPO_4, 286 mM NaCl, 1.4 mM KH_2PO_4, 2.6 mM KCl, 500 mM
305 imidazole and 0.1% sarkosyl (w/v), pH 7.4). 3 mg of purified protein were loaded onto a 12
306 % acrylamide prep-gel and dyed with Coomassie Brilliant Blue R-250. The protein band was
307 cut out and sent to ThermoFisher Scientific for antibody generation. For western blot analysis
308 the antiserum was diluted 1:250 in TBST containing 5% fish gelatine (Sigma) and detected
309 using an anti-rabbit IgG HRP-conjugated secondary antibody (Abcam) diluted 1:2000 in
310 gelatine/TBST.
311

312 **RESULTS**

313

314 **Sequence analyses suggest that *Tb*MCP17 is a mitochondrial iron transporter**

315 Genome database searches using the amino acid sequences of the functionally characterised
316 mitochondrial iron transporters from *S. cerevisiae* (MRS3 and MRS4) identified only one
317 homologue in the genome of *T. brucei*, *Tb*MCP17 (accession number Tb927.3.2980; [36]).
318 Reciprocal BLASTP analysis of eukaryotic protein databases (http://www.ncbi.nlm.nih.gov)
319 using the *Tb*MCP17 amino acid sequence retrieved mitochondrial iron transporters from
320 different species, including yeast MRS3 and MRS4, and mitoferrins from plants, mammals
321 and insects. Syntenic homologues are also present in all other kinetoplastids and the free-living
322 *Bodo saltans*; they include *Leishmania major* LmjF.29.2780 and *Trypanosoma cruzi*
323 TcCLB.508153.630, and TcCLB.510315.20.

324 The phylogenetic relationship of *Tb*MCP17 with mitochondrial iron carriers of other
325 eukaryotes was analysed using a neighbour-joining tree (Figure 1).

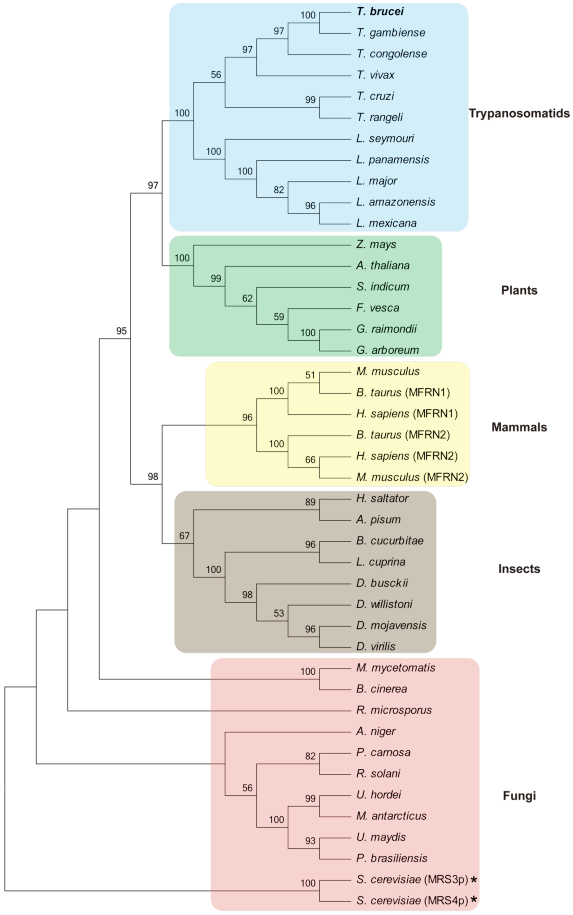

Figure 1. *Tb*MCP17 is evolutionarily related to mitochondrial iron transporters of the SLC25A family.

The evolutionary relationship was analysed using a Neighbour-Joining tree. The bootstrap consensus tree was obtained after resampling analysis of 1,000 reiterated data sets. Only significant bootstrap values (≥ 50%) are shown. Branches corresponding to partitions reproduced in less than 50% bootstraps are collapsed. *Tb*MCP17 is highlighted by bold face. Functionally characterised mitochondrial iron transporters are labelled with '*'. Corresponding accession numbers are indicated in the materials and methods section.

*Tb*MCP17 and homologous sequences from other trypanosomatids formed a well-defined, separate clade branching off near the iron carriers of plants with a well-resolved node and closely related to the mammalian mitoferrins and the iron carriers of insects. In mammals there

339 are two different isoforms of mitoferrins, MFRN1 and MFRN2 [31,54], forming two separate
340 branches within the mammalian clade and supported by high bootstrap values (Figure 1). As
341 expected, mitochondrial iron transporters from insects and mammals branched nearer to each
342 other than to the iron carriers from plants and trypanosomatids (Figure 1). Rather surprisingly,
343 instead of branching with the mammalian proteins, those from yeast formed an independent
344 group that was not supported by high bootstrap values (Figure 1).
345 The deduced amino acid sequence of *Tb*MCP17 consists of 289 amino acid residues, which
346 corresponds to a predicted molecular weight of 31.1 kDa (GeneDB). *Tb*MCP17 contains three
347 repetitive domains of about 100 amino acids, each harbouring two membrane-spanning alpha-
348 helices (Figure 2, H1-H6).

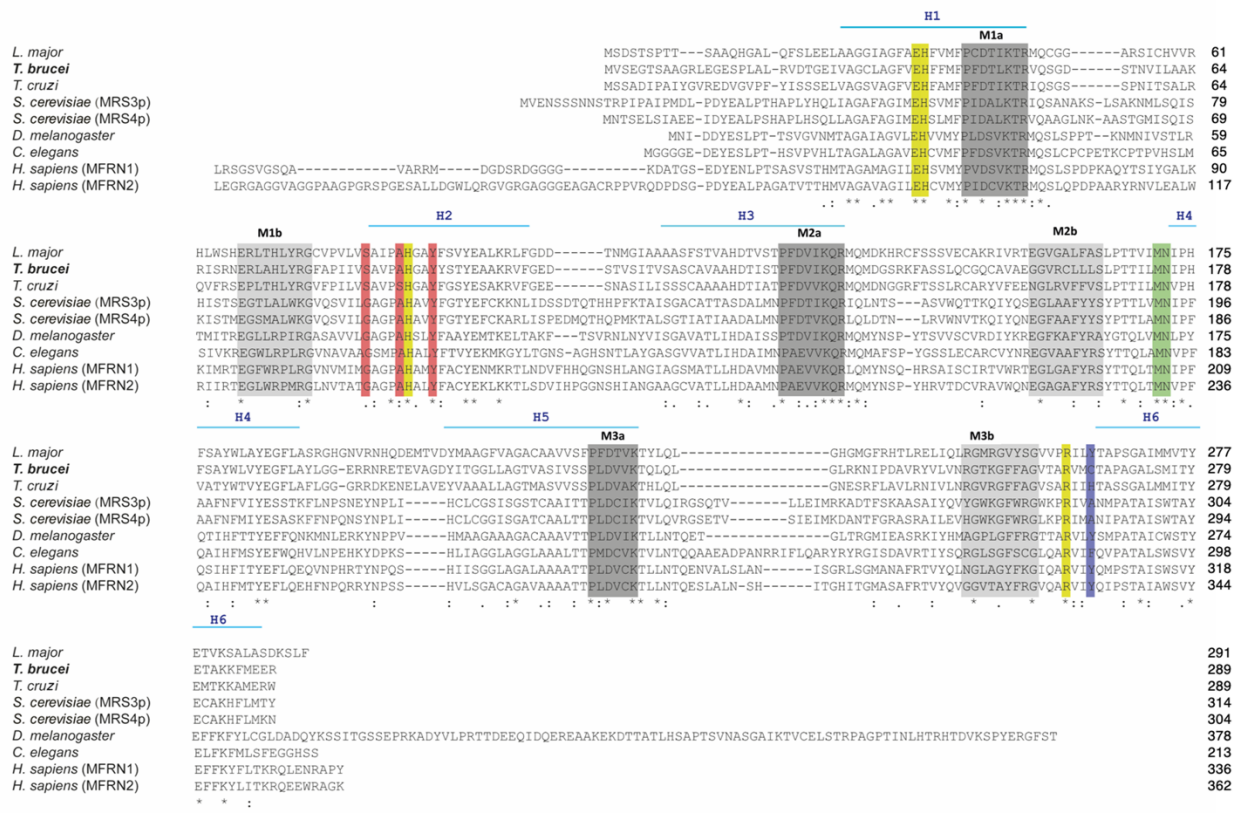

349

350

351 **Figure 2**. *Tb*MCP17 displays all conserved amino acid sequence features and functional
352 residues present in mitochondrial iron carriers.

353 Sequence alignment of *Tb*MCP17 with putative mitochondrial iron carrier sequences from
354 *Trypanosoma cruzi* and *Leishmania major*, MRS3p and MRS4p *Saccharomyces cerevisiae*
355 and mitoferrins from *Drosophila melanogaster*, *Caenorhabditis elegans* and *Homo sapiens*.
356 The six transmembrane helices are indicated using a blue line (H1-6). The first and second
357 part of the canonical signature sequence motifs are labelled with M1a, M2a and M3a, and
358 M1b, M2b and M3b and are shaded in dark and light grey respectively. Substrate contact points
359 are shaded in red (CPI), green (CPII) and blue (CPIII). The salt bridge networks are shaded in
360 yellow. (*) indicate fully conserved residues, (:) indicate strongly conserved (scoring >0.5 in
361 the Gonnet PAM 250 matrix), (.) indicate weakly conserved (scoring < 0.5 in the Gonnet PAM
362 250 matrix). Corresponding accession numbers are indicated in the materials and methods
363 section.
364
365 Characteristic for MCF proteins is a bipartite signature motif: the first part of the signature
366 motif (Px[D/E]x_2[K/R]x[K/R], x represents any residue) (Figure 2, M1a, M2a, and M3a) is
367 located at the carboxy-terminal end of the odd-numbered transmembrane helices, and the
368 second part of the signature motif ([D/E]G$x_{4\text{-}5}$[W/F/Y][K/R]G) (Figure 2, M1b, M2b, and
369 M3b) shortly before each even-numbered transmembrane helix, within an aliphatic loop [55–
370 57]. Multiple sequence alignments confirmed the conservation of the MCF-typical signature
371 sequences (M1a/M2a/M3a) in *Tb*MCP17 with some minor modifications (Figure 2). Within
372 the first part of the signature sequence the proline at position one, the aspartic acid at position
373 3 and the lysine at position 6 were conserved in *Tb*MCP17 (Figure 2). The positively charged
374 amino acid, either lysine or arginine, at position 8 was also conserved except in M3a (Figure
375 2). The second part of the sequence signature (M1b/M2b/M3b) was less conserved except for
376 the initial acidic residue (D or E) (Figure 2). In M1b the only substitution was at position 2
377 where glycine was substituted for arginine. In M2b the last 2 amino acids of the motif ([K/R]G)

378 and the preceding aromatic amino acid [W/F/Y] were not conserved in *Tb*MCP17. M3b was
379 little conserved and retained only the final glycine (Figure 2). The other aligned sequences
380 displayed similar levels of conservation in their signature motifs.
381 In MCF proteins the substrate specificity is determined by three well-conserved substrate-
382 contact points (CPI, CPII and CPIII) (marked respectively red, green and blue in Figure 2)
383 [35]. In *Tb*MCP17, like in all iron carriers, the amino acids constituting CPI and CPII are
384 [G/S]AY and MN respectively while CPIII is not conserved (Figure 2). Three further repetitive
385 clusters of conserved residues ([FY][DE]XX[RK]) located in H2, H4 and H6 (marked yellow
386 in Figure 2) are thought to be involved in the formation of salt bridge networks [58]. Except
387 for the last amino acid in the motif located in H4 the other repetitive clusters are well conserved
388 in all aligned sequences (Figure 2).
389
390 ***Tb*MCP17 complements growth in ΔMRS3/4 yeast**
391 To assess the function of *Tb*MCP17 as potential mitochondrial iron importer, functional
392 complementation was performed in ΔMRS3/4 *S. cerevisiae* strains (GW403). The wild type
393 and GW403 yeast strains were transfected using either empty pCM190 or pCM190 containing
394 *Tb*MCP17 or MRS3 and spotted on SCD (glucose) or SCG (glycerol) agar plates. The results
395 showed that GW403 yeast transfected with empty pCM190 grew slower than wild type yeast
396 or GW403 yeast complemented with either *Tb*MCP17 or MRS3 (Figure 3A). This effect was
397 particularly evident when the yeast was grown on glycerol instead of glucose as carbon source
398 (Figure 3A).
399

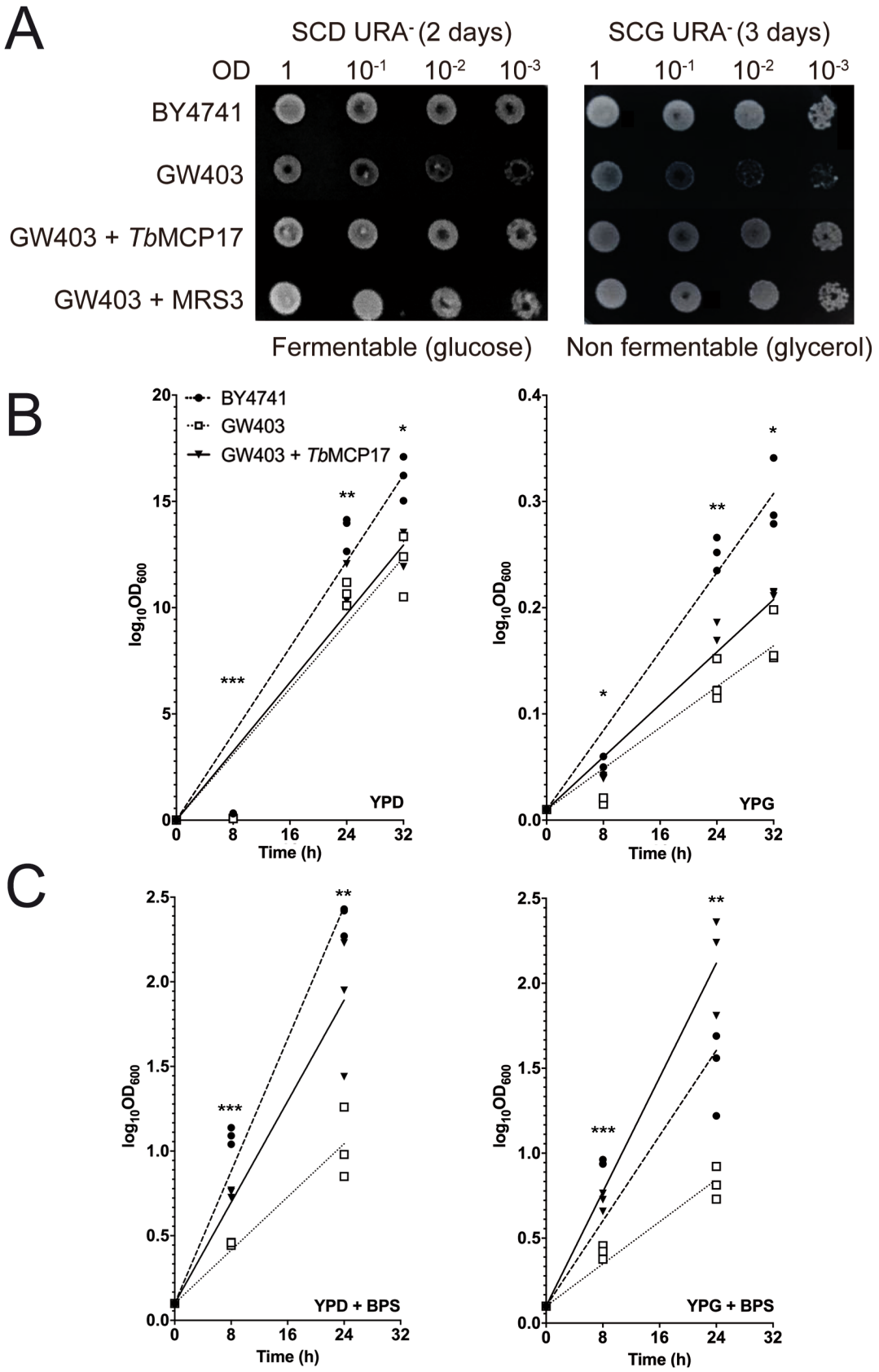

400

401 **Figure 3**. *Tb*MCP17 complements the growth defect of the ΔMRS3/4 yeast cell line.

402 **A.** The yeast strain BY4741 (wild-type) was transfected with empty pCM190 vector and the
403 yeast strain GW403 (ΔMRS3/4) was transfected with either empty pCM190 vector or with
404 pCM190 vector containing either the *Tb*MCP17 or the MRS3 ORF. Transfected yeast cells
405 were spotted in ten-fold dilutions on plates containing synthetic complete media without uracil
406 supplemented with either dextrose (SCD URA^-) or glycerol (SCG URA^-). **B.** and **C.** The yeast
407 strain BY4741 (wild-type) was transfected with empty pCM190 vector and the yeast strain
408 ΔMRS3/4 was transfected with either empty pCM190 vector or with pCM190 vector
409 containing the *Tb*MCP17 ORF. Transfected cells were grown either in standard YPD or YPG
410 (**B**) or YPD or YPG supplemented with 80 µM bathophenanthrolinedisulfonic acid (BPS) (**C**).
411 For each yeast strain three individual growth curves were plotted. Statistical significance was
412 determined by one-way ANOVA using GraphPad Prism 7: *: $p \leq 0.05$ **: $p \leq 0.01$; ***$p \leq$
413 0.001.
414
415 Next, the growth rates of the different yeast strains were analysed in YPD (glucose), YPG
416 (glycerol), YPD/BPS (glucose and iron chelator) and YPG/BPS (glycerol and iron chelator)
417 suspension culture media over a period of 32 h or 24 h (for experiments with BPS). The best
418 growth rate for all tested yeast cell lines was observed on YPD medium. In this medium no
419 difference in growth was observed between ΔMRS3/4 cells transfected with either *Tb*MCP17
420 or empty vector, which all grew slightly slower than the wild type strain (Figure 3B). In YPG
421 media, the ΔMRS3/4 and the ΔMRS3/4 cell line transfected with empty vector grew
422 significantly slower than wild type cells (Figure 3B). Transfection of the ΔMRS3/4 line with
423 *Tb*MCP17 partially rescued the growth to normal levels compared to the strain transfected
424 with empty vector (Figure 3B). The addition of the iron chelator BPS resulted in drastically
425 reduced growth rates for all strains on YPD and YPG medium compared with the growth
426 without iron chelator (Figure 3C). However, in both media containing BPS, *Tb*MCP17

427 improved the growth of the ΔMRS3/4 strain relatively to the strain transfected with empty
428 vector (Figure 3C). Taken together these results demonstrated that *Tb*MCP17 partially restores
429 growth of the ΔMRS3/4 strain by complementing the transport function of the yeast iron
430 carriers.
431

432 ***Tb*MCP17 localises to the mitochondrion of PCF *T. brucei***

433 Results from one of our previous publications demonstrated that the iron carrier, together with
434 the dicarboxylate carrier *Tb*MCP12, are the only *T. brucei* MCF carriers to be differentially
435 expressed at the mRNA level [36,39]. Since those results showed that *Tb*MCP17 is
436 approximately 2-fold higher expressed in PCF than in BSF [36] and because we did not obtain
437 viable BSF clones over expressing *Tb*MCP17, in the current work we focussed on its
438 functional characterisation in PCF only.
439 Several attempts to detect endogenous *Tb*MCP17 in PCF using the antibody we generated
440 were not successful, although the antibody readily detected *Tb*MCP17 in PCF when the protein
441 was overexpressed (Supplementary Figure S1). When using our standard culturing conditions
442 *Tb*MCP17 was therefore below the detection limit of the antibody.

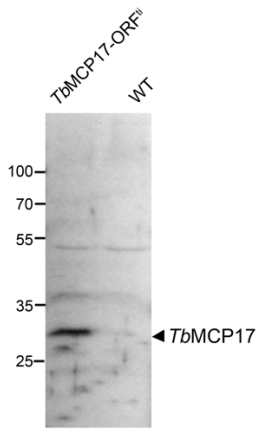

443

444 **Supplementary Figure S1.** Western blot analysis of *Tb*MCP17 using the antibody we
445 generated in wild type PCF and PCF overexpressing *Tb*MCP17. In each lane 10 µl of sample
446 containing $5x10^6$ cells were loaded.
447
448 Since the location of mitochondrial targeting sequences in proteins belonging to the SLC25A
449 protein family has not been fully clarified yet [59–61] we assessed the subcellular localisation
450 of *Tb*MCP17 by over-expressing it bearing either a C-terminal or N-terminal myc-tag in PCF
451 (MCP17-cmyc^{ti} and MCP17-nmyc^{ti}). In this way we ensure that the myc-tag is not interfering
452 with the mitochondrial localisation of the protein. Following transfection of PCF *T. brucei*
453 with the over expression constructs, western blot analysis using an antibody directed against
454 the myc-tag showed a band of approximately 33 kDa for both the *Tb*MCP17-cmyc^{ti} and the
455 *Tb*MCP17-nmyc^{ti} PCF cell lines, but not for the wild type cells (Figure 4A). Leakiness of the
456 tet-inducible expression-system in the absence of tetracycline [39,48] was not detectable by
457 western blotting but cannot be excluded. Therefore wild-type cells were used as control cell-
458 line in all experiments. Immunofluorescence analysis using Mitotracker and an antibody
459 directed against the myc-tag showed that both N- and C-terminally tagged *Tb*MCP17 are
460 localised to the mitochondrion (Figure 4B).

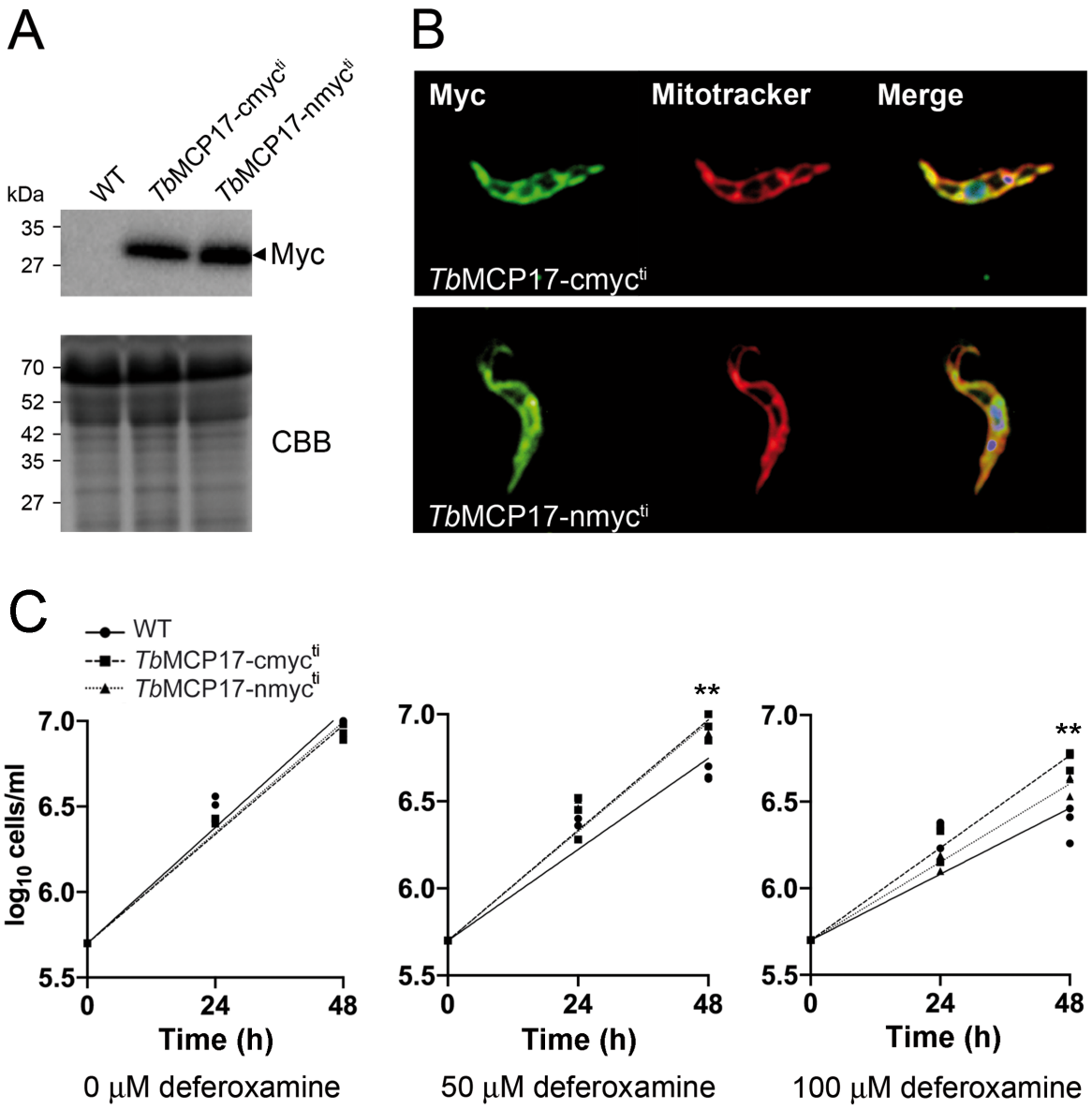

461

462 **Figure 4**. In PCF *Tb*MCP17 is localised in the mitochondrion and its overexpression confers

463 increased resistance to iron depletion.

464 **A**. Western blot analysis of WT PCF and PCF over-expressing *Tb*MCP17 with either C-term

465 (*Tb*MCP17-cmyc^{ti}) or N-term myc-tag (*Tb*MCP17-nmyc^{ti}). Coomassie brilliant blue (CBB) is

466 used as loading control. **B.** Immunofluorescence analysis of PCF over expressing *Tb*MCP17

467 bearing either C-term (*Tb*MCP17-cmyc^{ti}) or N-term myc-tag (*Tb*MCP17-nmyc^{ti}).

468 Mitochondria were visualised using Mitotracker (red) and *Tb*MCP17-myc was detected using

469 a 1:1000 dilution of a myc antibody (green). Nucleus and kinetoplasts are stained with DAPI
470 (blue). **C.** Growth analysis of PCF wild-type (WT), *Tb*MCP17-cmyc^{ti} and *Tb*MCP17-nmyc^{ti}
471 cells in the absence and presence of the iron chelator deferoxamine. The growth experiment
472 was started at a cell density of 0.5×10^6 cells/ml and cells were counted every 24 h for a period
473 of 48 h. In some experiments, cells were treated with either 50 or 100 µM deferoxamine. For
474 each cell-line three individual growth curves were plotted. Statistical significance was
475 determined by one-way ANOVA using GraphPad Prism 7: *: $p \leq 0.05$ **: $p \leq 0.01$; ***$p \leq$
476 0.001.
477
478 **Over expression of *Tb*MCP17 sustains growth under iron-limiting condition in PCF *T.***
479 ***brucei***
480 To investigate whether a surplus of *Tb*MCP17 enabled better survival of *T. brucei* under iron-
481 limiting conditions *Tb*MCP17-cmyc^{ti} and *Tb*MCP17-nmyc^{ti} procyclic cell lines were
482 cultivated in medium containing different concentrations of the iron chelator deferoxamine.
483 Deferoxamine is a conventionally used and well-established compound for blocking iron
484 uptake in trypanosomes [62]. In contrast to BPS, it is membrane-permeable and chelates
485 intracellular iron thereby blocking its incorporation into newly synthesized proteins [62]. In
486 medium containing no deferoxamine, *Tb*MCP17-cmyc^{ti} and *Tb*MCP17-nmyc^{ti} cells doubled
487 at the same speed as wild type cells (Figure 4C). The division time of wild type cells when
488 exposed to 50 µM or 100 µM deferoxamine for 48 h was significantly slowed down compared
489 to the cells overexpressing *Tb*MCP17 (respectively $p = 0.0012$ and $p = 0.0031$) or untreated
490 cells (respectively $p = 0.0012$ and $p = 0.0042$) (Figure 4C). Instead, the division time of
491 *Tb*MCP17-cmyc^{ti} and *Tb*MCP17-nmyc^{ti} was not affected by the exposure to 50 µM iron
492 chelator and only slightly but not significantly slowed down when exposed to 100 µM iron

493 chelator (Figure 4C). These results indicate that the overexpression of *Tb*MCP17 confers
494 increased resistance to iron depletion.
495
496 ***Tb*MCP17 is required to sustain normal growth of PCF *T. brucei***
497 We were next interested to investigate whether *Tb*MCP17 was essential for procyclic *T. brucei*
498 viability. To deplete *TbMCP17* we used two different approaches: conditional gene knock out
499 and RNA interference (RNAi).
500 For the conditional gene knock out we replaced the two alleles of *TbMCP17* with antibiotic
501 resistant cassettes in the background of the tetracycline inducible *Tb*MCP17-cmyc^{ti} generating
502 the cell-line Δ*Tb*MCP17/*Tb*MCP17-cmyc^{ti} according to the previously published method [37–
503 39]. PCR using different primer sets located along the modified *TbMCP17* gene locus
504 (Supplementary Table 1) was performed to confirm the removal of the *TbMCP17* gene and
505 the correct insertion of the resistance cassettes (Supplementary Figure 2).
506

Primer number	Primer name	Primer sequence
427	MCP17upstreamFor	gatgatcgtatcggctcttgtcgcaatg
339	MCP17KO5ForSac	gctagagctccgtgtcgtgaggtggagaggtgatg
429	NEOFor	atgcggcggctggatacggttg
82	BSDFor	atggccaagcctttgtctcaagaagaatccac
83	BSDRev	ttagccctcccacacataaccagagg
105	NeoRev	tcagaagaactcgtcaagaaggcgatagaag
430	NeoRev2	cgagcccctgatgctcttcgtccagatcatcctgatc
431	MCP17downstreamRev	aaggagtgggaacaggggcaaatccac
338	MCP17KO3RevA	ctatgggcccgtcaaacacattactggagcgg

507 **Supplementary Table 1**. Primers used for checking the correct integration of the knock out
508 construct.
509

A

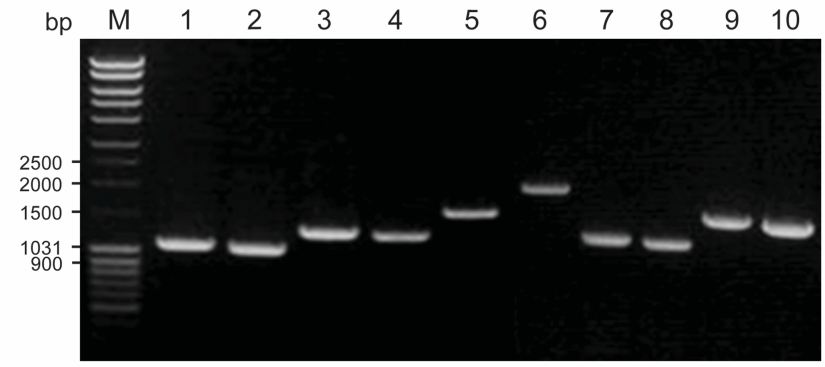

B

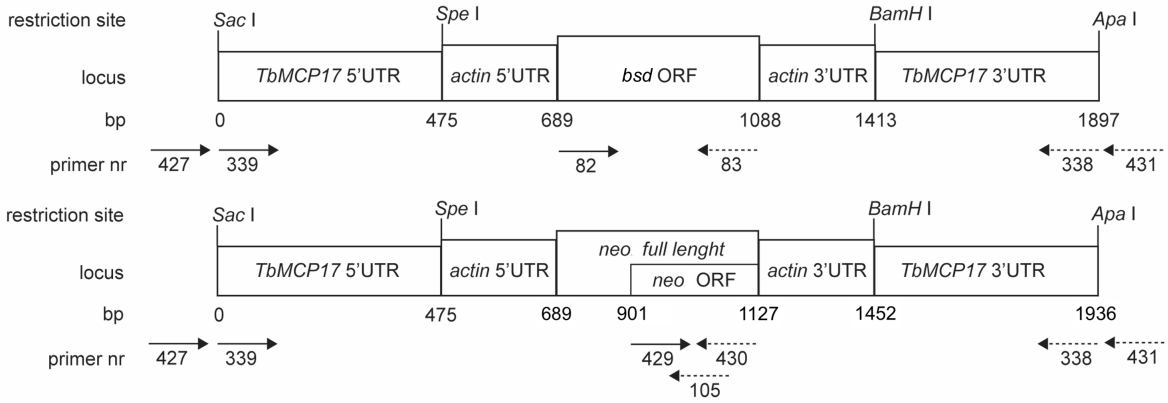

C

PCR number	Forward primer	Reverse primer	Predicted product size (bp)
1	427	83	1116
2	339	83	1088
3	427	105	1079
4	339	105	1051
5	427	430	1155
6	339	431	1964
7	429	431	1062
8	429	338	1035
9	82	431	1235
10	82	338	1208

510

511 **Supplementary Figure 2**. PCR analysis of the correct integration of the antibiotic resistance

512 cassette in the Δ*Tb*MCP17/*Tb*MCP17-cmyc^{ti} cell-line. **A.** gDNA derived from

513 Δ*Tb*MCP17/*Tb*MCP17-cmyc^{ti} was PCR amplified and loaded on a 0.5% agarose gel together

514 with a DNA ladder. **B**. Schematic representation of the location of the primers used in A.

515 within the recombination site at the *Tb*MCP17 gene locus. **C.** List of the primers used in A.
516 and their predicted PCR amplified DNA fragment size.
517
518 To check the correct integration of the antibiotic resistance cassettes, primers located upstream
519 (427) and downstream (431) of the homologous recombination site were used in combination
520 with primers located in the BSD (82 and 83) or NEO (105, 429, 430) ORFs (Supplementary
521 Figure 2 C). All PCRs performed using genomic DNA derived from the *Tb*MCP17 knock out
522 cells produced a fragment of the predicted length confirming the integration of the resistance
523 genes in the *Tb*MCP17 locus (Supplementary Figure 2 A and C). Tetracycline removal from
524 the culture depletes the myc-tagged *Tb*MCP17 (Figure 5A). This cell line was referred to as
525 *Tb*MCP17-cmyc^{ti} depleted knock out (*Tb*MCP17 KO).

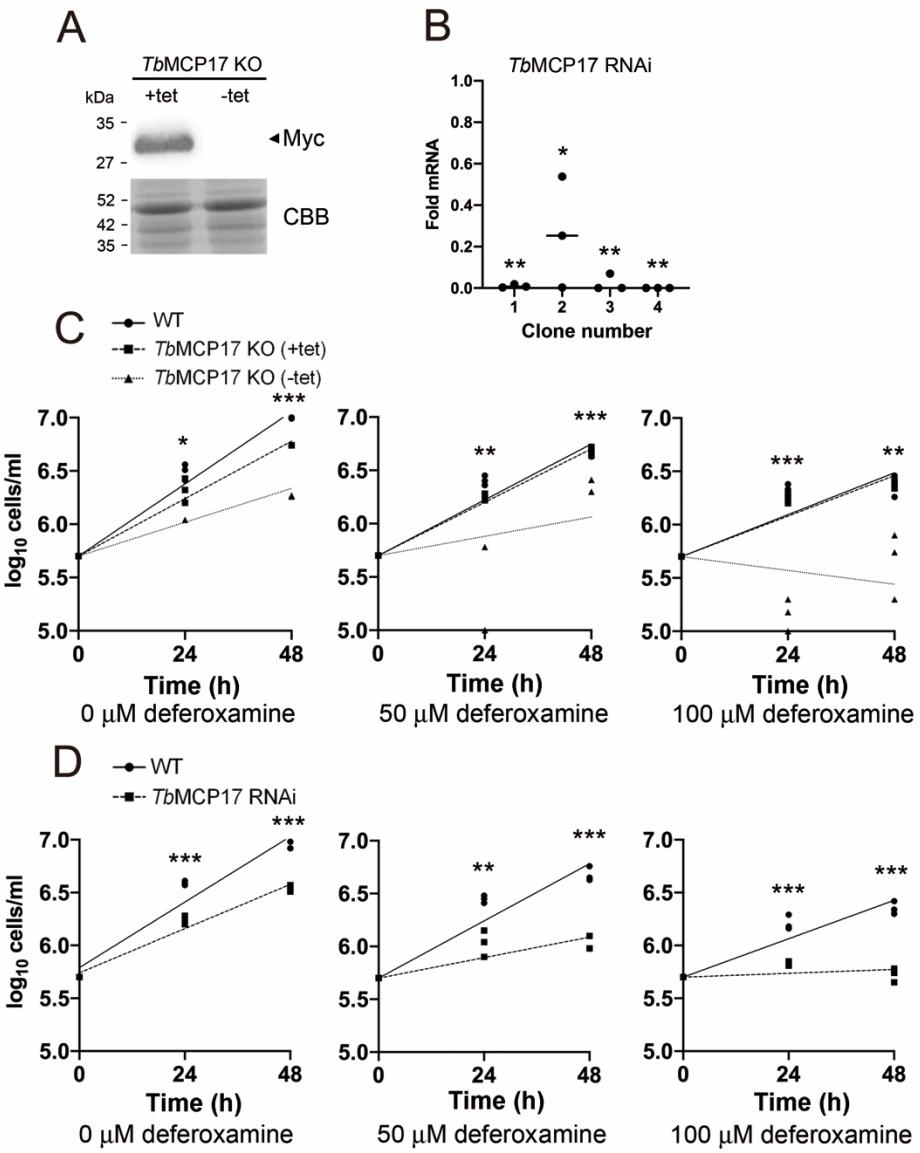

526

527 **Figure 5**. *Tb*MCP17 depletion impairs PCF *T. brucei* growth and renders the cells more

528 susceptible to iron depletion.

529 **A.** Western blot analysis of *Tb*MCP17 KO grown in the presence and absence of tetracycline

530 for 48 h. Coomassie brilliant blue (CBB) is used as loading control. **B.** qPCR analysis of the

531 *Tb*MCP17 expression of 4 different *Tb*MCP17 RNAi clones harvested after 48 h of growth in

532 the presence of tetracycline. *Tb*MCP17 expression of WT PCF was set to 1. Graph represents

533 the mean of 3 independent experimental replicates and individual values are plotted. Statistical

534 significance was determined by one-way ANOVA using GraphPad Prism 7: *: $p \leq 0.05$ **: p

535 ≤ 0.01; ***$p \leq 0.001$. **C.** and **D.** Growth analysis of PCF wild-type (WT) and *Tb*MCP17 KO

536 (+ and – tet) PCF cells (**C**) or *Tb*MCP17 RNAi PCF cells (**D**) in the absence or presence of the
537 iron chelator deferoxamine. The analysis of the growth curve was started at a cell density of
538 $0.5x10^6$ cells/ml and cells were counted every 24 h for a period of 48 h. In some experiments,
539 cells were treated with either 50 or 100 µM deferoxamine. For each cell-line three individual
540 growth curves were plotted. Statistical significance was determined by one-way ANOVA
541 using GraphPad Prism 7: *: $p \leq 0.05$ **: $p \leq 0.01$; ***$p \leq 0.001$.
542
543 The efficacy of 4 *Tb*MCP17 RNAi clones was tested using RT-qPCR. Compared to wildtype
544 cells, in three clones we found over 100-fold reduction of the mRNA expression of *Tb*MCP17
545 (clones 1, 3 and 4), while in one (clone 2) only 4-fold reduction was achieved (Figure 5B).
546 In medium containing no deferoxamine, the doubling time of the *Tb*MCP17-cmyc^{ti} depleted
547 KO was significantly slowed down compared to either wild type or induced *Tb*MCP17 KO
548 (Figure 5C). A similar increase in doubling time compared to wild type cells was obtained
549 when *Tb*MCP17 was depleted by RNAi when no iron chelator was added to the culture (Figure
550 5D).
551 The doubling time in iron-depleting conditions (50 or 100 µM deferoxamine) was significantly
552 slowed down in the *Tb*MCP17-cmyc^{ti} depleted KO cells compared to wild type cells and
553 induced *Tb*MCP17 KO cells (Figure 5C). The *Tb*MCP17-cmyc^{ti} depleted KO, however,
554 displayed a slight recovery after 48 h in culture. Like the *Tb*MCP17-cmyc^{ti} depleted KO, also
555 the *Tb*MCP17 RNAi cells displayed significantly increased sensitivity to iron depletion
556 (Figure 5D)
557
558 **Mitochondrial iron content is decreased in *Tb*MCP17 depleted cells**
559 We next measured the iron content of total cell lysates and isolated mitochondria in wild type,
560 *Tb*MCP17cmyc^{ti} and *Tb*MCP17 RNAi cell lines. In standard medium, wild type and

561 *Tb*MCP17cmyc^{ti} cells presented similar iron content in both whole cell lysates and
562 mitochondria as well as comparable iron distribution percentage (Fe_{mito}:Fe_{total}) (Figure 6A and
563 C). *Tb*MCP17 RNAi cell lines instead presented a slight, though not significant increment of
564 the whole cell iron content compared to wild type and *Tb*MCP17cmyc^{ti} cells, while the
565 mitochondrial iron content was unchanged.
566

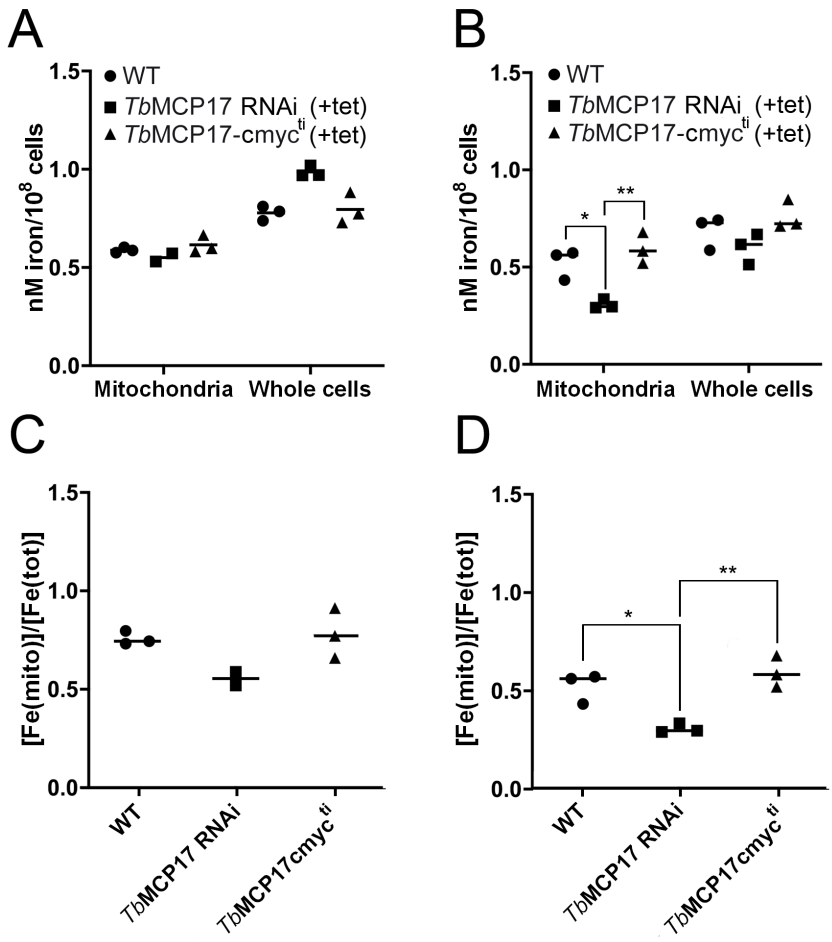

567

568 **Figure 6.** Mitochondrial iron content is reduced by the depletion of *Tb*MCP17 only under iron
569 limiting conditions.

570 **A.** and **B**. The iron content was measured in whole cell extracts and isolated mitochondria
571 derived from 1×10^8 WT, *Tb*MCP17cmyc^{ti} and *Tb*MCP17 RNAi PCF cells, which were
572 cultivated in normal (**A**) or heme-depleted medium (**B**). **C.** and **D.** Iron distribution

573 (Fe_{mito}:Fe_{total}) in WT, *Tb*MCP17cmyc^{ti} and *Tb*MCP17 RNAi PCF cells, which were cultivated
574 in normal (**C**) or heme-depleted medium (**D**) medium. All graphs (A, B, C and D) were derived
575 from 3, separately plotted, experiments. Statistical significance was determined by one-way
576 ANOVA using GraphPad Prism 7: *: $p \leq 0.05$ **: $p \leq 0.01$; ***$p \leq 0.001$.
577
578 Trypanosomes are auxotrophic for heme [63,64]. After heme removal the iron content was
579 significantly decreased only in isolated mitochondria of cells in which *Tb*MCP17 was depleted
580 (Figure 6B). The *Tb*MCP17 RNAi cell-line also displayed a significantly lower iron
581 distribution percentage compared with wild type cells and cells overexpressing
582 *Tb*MCP17cmyc^{ti} (Figure 6D).

583 **DISCUSSION**

584

585 The aim of this study was the identification of the carrier that is involved in the transport of
586 iron across the inner mitochondrial membrane of the parasite *T. brucei*. Our results show that
587 the *T. brucei* gene *TbMCP17,* which codes for a member of the SLC25A mitochondrial carrier
588 family is the only homologue of mitochondrial iron transporters present in the genome of this
589 parasite. Phylogenetic and amino acid sequence analysis demonstrated that *Tb*MCP17 is
590 closely related to the iron transporters of plants, insects and mammals and displays all
591 signature motifs and residues typically found in mitochondrial iron carriers. It is interesting
592 that as we previously reported for the mitochondrial dicarboxylate carrier *Tb*MCP12 [39] also
593 *Tb*MCP17 appears to have a closer phylogenetic relationship to plant transporters than to those
594 of Opisthokonts, although Excavata probably diverged equally early from both. Also, several
595 *T. brucei* enzymes such as fructose-1,6-bisphosphate aldolase and arginine kinases were
596 proposed to have arisen through horizontal gene transfer from either cyanobacteria, algae,
597 plants or insects [39,65–68].

598 *Tb*MCP17 successfully rescued the growth defect of the ΔMRS3/4 (GW403) yeast strain on
599 non-fermentable carbon sources. This observation strongly suggested that *Tb*MCP17 can
600 partially complement the function of yeast MRS3 and MRS4 on non-fermentable carbon
601 sources by translocating iron into the mitochondrial matrix. Yeast growth was, however, never
602 fully restored to wild type levels; perhaps amino acid sequence variations present in *Tb*MCP17
603 impair either its correct integration into the yeast mitochondrial inner membrane or the kinetics
604 of the transport activity. Similar observations were already reported for the carrier *Tb*MCP12
605 [39].

606 In procyclic *T. brucei*, growth under iron limiting conditions was significantly improved when
607 *Tb*MCP17 was over-expressed, while down-regulation and knock out of *Tb*MCP17

608 significantly reduced cell viability and caused hypersensitivity to iron deprivation. Similar
609 susceptibility was previously observed when the mucolipin-like protein (*Tb*MLP), an
610 endosomal channel required for the assimilation of iron, was depleted from BSF *T. brucei* [14].
611 After 48 h of growth on deferoxamine we observed a partial recovery of the growth phenotype
612 in the *Tb*MCP17-cmyc^{ti} depleted KO. Reasons for this observation might be: i) metabolic
613 adjustments that compensate the decreased iron availability, ii) the upregulation of the
614 expression of other mitochondrial carriers involved in iron transport eg. *Tb*MCP23 or
615 sideroflexins (*Tb*SFNX). *Tb*MCP23 is highly homologous to Rim2 [36], which mediates the
616 translocation of iron and other divalent metal ions across the mitochondrial inner membrane.
617 In yeast, the combined removal of Mrs3, Mrs4, and Rim2 caused a more severe Fe-S protein
618 maturation defect than the depletion of the Mrs proteins alone [45]. Sideroflexins were
619 identified in *T. brucei* and display high sequence similarity to the tricarboxylate transporter
620 SLC25A1 (C. Colasante, unpublished data). The depletion of these proteins causes iron
621 accumulation in mitochondria and siderocytic anaemia in mice [69,70], indicating their
622 potential role in iron transport, iii) Selective pressure caused by the low iron concentration
623 might exacerbate the leakiness of the tetracycline-inducible system generating sufficiently
624 high amounts of *Tb*MCP17 to improve growth though remaining under the detection limit of
625 the western blot analysis.
626 Our results suggested that iron storage is disturbed when *Tb*MCP17 is absent and enhanced
627 when its abundance is increased. When we analysed the iron content of total cell lysates of
628 procyclic *T. brucei* we found, however, that the mitochondrial iron content and the
629 Fe(mito)/Fe(total) ratio were significantly lowered in *Tb*MCP17 RNAi cells under low iron
630 conditions but never significantly elevated when *Tb*MCP17 was overexpressed. This indicated
631 that *Tb*MCP17 downregulation decreased, as expected, mitochondrial iron import, which
632 further substantiates its function as iron carrier. That *Tb*MCP17 overexpression does not

633 increase mitochondrial iron storage in either normal or iron depleted conditions might be due
634 to regulatory mechanisms that limit mitochondrial iron import. It was indeed previously shown
635 that over expression of Mfrn1 and Mfrn2 did not increase mitochondrial iron depots in
636 mammalian cells and that mitochondria modulate their own iron import [71,72]
637 Several reports showed that in yeast the depletion of MRS3 and MRS4 did not change iron
638 accumulation within mitochondria or the activity of the iron sulphur proteins aconitase and
639 succinate dehydrogenase, except when the cells were deprived of iron [28,30]. The authors
640 concluded that when iron is available other iron transport systems are supplying the
641 mitochondrion and that MRS3 and MRS4 are only active when iron was low abundant [28,30].
642 In contrast, in mammalian cells, the knock out of Mrfn1 and Mrfn2 abolished mitochondrial
643 iron import even when iron was provided to the medium[73]. Another study reported that the
644 depletion of MRS3 and MRS4 induced the yeast iron regulon and led to an increased iron
645 uptake into the cytoplasm and vacuole [73]. In rice shoots the depletion of the plant iron carrier
646 MIT caused an elevation of intracellular, but a reduction of mitochondrial, iron content [74].
647 It appears that the regulation of the intracellular iron distribution in *T. brucei* is similar to that
648 in yeast. Although, unlike yeast, *T. brucei* does not possess a vacuole, excess iron might be
649 stored within a yet unidentified depot and released when cytosolic concentrations are below a
650 certain threshold level [75]. It was previously suggested that this putative iron store could
651 support the parasite´s growth for up to 48 h when iron is absent from the culture medium or
652 when iron import to the cytoplasm is blocked [14,76,77].
653 Taken together with the phylogenetic and the sequence analysis, our results suggest that
654 *Tb*MCP17 acts as a mitochondrial iron carrier in *T. brucei*. We further propose that this carrier
655 is particularly relevant for mitochondrial iron transport when iron is not readily available from
656 the environment.
657

658 **References**

659 [1] J. Rodgers, Human African trypanosomiasis, chemotherapy and CNS disease, J.
660 Neuroimmunol. (2009). doi:10.1016/j.jneuroim.2009.02.007.
661 [2] M.P. Barrett, R.J. Burchmore, A. Stich, J.O. Lazzari, A.C. Frasch, J.J. Cazzulo, S.
662 Krishna, The trypanosomiases, Lancet. (2003). doi:10.1016/S0140-6736(03)14694-
663 6.
664 [3] D. Moreira, P. López-García, K. Vickerman, An updated view of kinetoplastid
665 phylogeny using environmental sequences and a closer outgroup: Proposal for a new
666 classification of the class Kinetoplastea, Int. J. Syst. Evol. Microbiol. (2004).
667 doi:10.1099/ijs.0.63081-0.
668 [4] R. Sharma, E. Gluenz, L. Peacock, W. Gibson, K. Gull, M. Carrington, The heart of
669 darkness : growth and form of *Trypanosoma brucei* in the tsetse fly, 25 (2009) 517–
670 524. doi:10.1016/j.pt.2009.08.001.
671 [5] A.G.M. Tielens, J.J. Van Hellemond, Differences in energy metabolism between
672 Trypanosomatidae, Parasitol. Today. 14 (1998) 265–271. doi:10.1016/S0169-
673 4758(98)01263-0.
674 [6] P.A.M. Michels, F. Bringaud, M. Herman, V. Hannaert, Metabolic functions of
675 glycosomes in trypanosomatids, Biochim. Biophys. Acta - Mol. Cell Res. 1763
676 (2006) 1463–1477. doi:10.1016/j.bbamcr.2006.08.019.
677 [7] P.A.M. Michels, V. Hannaert, F. Bringaud, Metabolic aspects of glycosomes in
678 Trypanosomatidae - New data and views, Parasitol. Today. 16 (2000) 482–489.
679 doi:10.1016/S0169-4758(00)01810-X.
680 [8] V. Coustou, S. Besteiro, M. Biran, P. Diolez, V. Bouchaud, P. Voisin, P.A.M.
681 Michels, P. Canioni, T. Baltz, F. Bringaud, ATP generation in the *Trypanosoma*
682 *brucei* procyclic form: cytosolic substrate level is essential, but not oxidative

683 phosphorylation., J. Biol. Chem. 278 (2003) 49625–49635.
684 doi:10.1074/jbc.M307872200.
685 [9] A.G.M. Tielens, New functions for parts of the krebs cycle in procyclic,
686 Biochemistry. 280 (2005) 12451–12460. doi:10.1074/jbc.M412447200.
687 [10] S. Besteiro, M.P. Barrett, L. Rivière, F. Bringaud, Energy generation in insect stages
688 of *Trypanosoma brucei*: Metabolism in flux, Trends Parasitol. 21 (2005) 185–191.
689 doi:10.1016/j.pt.2005.02.008.
690 [11] Z. Verner, S. Basu, C. Benz, S. Dixit, E. Dobáková, D. Faktorová, H. Hashimi, E.
691 Horáková, Z. Huang, Z. Paris, P. Peña-Diaz, L. Ridlon, J. Týč, D. Wildridge, A.
692 Zíková, J. Lukeš, Malleable mitochondrion of Trypanosoma brucei, Int. Rev. Cell
693 Mol. Biol. 315 (2015) 73–151. doi:10.1016/bs.ircmb.2014.11.001.
694 [12] S. Basu, E. Horáková, J. Luke, Biochim. Biophys. Acta Iron-associated biology of
695 *Trypanosoma brucei*, 1860 (2016) 363–370. doi:10.1016/j.bbagen.2015.10.027.
696 [13] D. Steverding, The transferrin receptor of *Trypanosoma brucei*, Parasitol. Int.
697 (2000). doi:10.1016/S1383-5769(99)00018-5.
698 [14] M.C. Taylor, A.P. Mclatchie, J.M. Kelly, Evidence that transport of iron from the
699 lysosome to the cytosol in African trypanosomes is mediated by a mucolipin
700 orthologue, 89 (2013) 420–432. doi:10.1111/mmi.12285.
701 [15] B. Vanhollebeke, G. De Muylder, M.J. Nielsen, A. Pays, P. Tebabi, M. Dieu, M.
702 Raes, S.K. Moestrup, E. Pays, A haptoglobin-hemoglobin receptor conveys innate
703 immunity to *Trypanosoma brucei* in humans, Science (2008).
704 doi:10.1126/science.1156296.
705 [16] J. Mach, J. Tachezy, R. Sutak, Efficient Iron Uptake via a Reductive Mechanism in
706 Procyclic *Trypanosoma brucei* , J. Parasitol. (2013). doi:10.1645/ge-3237.1.
707 [17] J. Lukeš, S. Basu, Fe/S protein biogenesis in trypanosomes - A review, Biochim.

708 Biophys. Acta - Mol. Cell Res. (2015). doi:10.1016/j.bbamcr.2014.08.015.
709 [18] M. Dormeyer, R. Schoneck, G.A. Dittmar, R.L. Krauth-Siegel, Cloning, sequencing
710 and expression of ribonucleotide reductase R2 from *Trypanosoma brucei*, FEBS
711 Lett. (1997). doi:S0014-5793(97)01036-3 [pii].
712 [19] A. Hofer, P.P. Schmidt, A. Gräslund, L. Thelander, Cloning and characterization of
713 the R1 and R2 subunits of ribonucleotide reductase from *Trypanosoma brucei*, Proc.
714 Natl. Acad. Sci. U. S. A. (1997). doi:10.1073/pnas.94.13.6959.
715 [20] N. Le Trant, S.R. Meshnick, K. Kitchener, J.W. Eaton, A. Cerami, Iron-containing
716 superoxide dismutase from Crithidia fasciculata. Purification, characterization, and
717 similarity to Leishmanial and trypanosomal enzymes., J. Biol. Chem. (1983).
718 [21] A.B. Clarkson, E.J. Bienen, G. Pollakis, R.W. Grady, Respiration of bloodstream
719 forms of the parasite *Trypanosoma brucei brucei* is dependent on a plant-like
720 alternative oxidase, J. Biol. Chem. (1989).
721 [22] A. Tsuda, W.H. Witola, K. Ohashi, M. Onuma, Expression of alternative oxidase
722 inhibits programmed cell death-like phenomenon in bloodstream form of
723 *Trypanosoma brucei rhodesiense*, Parasitol. Int. (2005).
724 doi:10.1016/j.parint.2005.06.007.
725 [23] A. Tsuda, W.H. Witola, S. Konnai, K. Ohashi, M. Onuma, The effect of TAO
726 expression on PCD-like phenomenon development and drug resistance in
727 *Trypanosoma brucei*, Parasitol. Int. (2006). doi:10.1016/j.parint.2006.01.001.
728 [24] P. Overath, J. Czichos, C. Haas, The effect of citrate/cis-aconitate on oxidative
729 metabolism during transformation of *Trypanosoma brucei*, Eur. J. Biochem. (1986).
730 doi:10.1111/j.1432-1033.1986.tb09955.x.
731 [25] M.C. Taylor, J.M. Kelly, Iron metabolism in trypanosomatids, and its crucial role in
732 infection, Parasitology. 137 (2010) 899–917. doi:10.1017/S0031182009991880.

733 [26] A. Tangerås, T. Flatmark, D. Bäckström, A. Ehrenberg, Mitochondrial iron not
734 bound in heme and iron-sulfur centers. Estimation, compartmentation and redox
735 state, BBA - Bioenerg. (1980). doi:10.1016/0005-2728(80)90035-3.
736 [27] T.A. Rouault, W.H. Tong, Iron-sulphur cluster biogenesis and mitochondrial iron
737 homeostasis, Nat. Rev. Mol. Cell Biol. (2005). doi:10.1038/nrm1620.
738 [28] F. Foury, T. Roganti, Deletion of the mitochondrial carrier genes MRS3 and MRS4
739 suppresses mitochondrial iron accumulation in a yeast frataxin-deficient strain, J.
740 Biol. Chem. 277 (2002) 24475–24483. doi:10.1074/jbc.M111789200.
741 [29] M.R. Felice, I. De Domenico, L. Li, D.M. Ward, B. Bartok, G. Musci, J. Kaplan,
742 Post-transcriptional regulation of the yeast high affinity iron transport system., J.
743 Biol. Chem. (2005). doi:10.1074/jbc.M414663200.
744 [30] U. Mühlenhoff, J.A. Stadler, N. Richhardt, A. Seubert, T. Eickhorst, R.J. Schweyen,
745 R. Lill, G. Wiesenberger, A Specific Role of the Yeast Mitochondrial Carriers
746 Mrs3/4p in Mitochondrial Iron Acquisition under Iron-limiting Conditions, J. Biol.
747 Chem. 278 (2003) 40612–40620. doi:10.1074/jbc.M307847200.
748 [31] G.C. Shaw, J.J. Cope, L. Li, K. Corson, C. Hersey, G.E. Ackermann, B. Gwynn, A.J.
749 Lambert, R.A. Wingert, D. Traver, N.S. Trede, B.A. Barut, Y. Zhou, E. Minet, A.
750 Donovan, A. Brownlie, R. Balzan, M.J. Weiss, L.L. Peters, J. Kaplan, L.I. Zon, B.H.
751 Paw, Mitoferrin is essential for erythroid iron assimilation, Nature. (2006).
752 doi:10.1038/nature04512.
753 [32] H. Aquila, T.A. Link, M. Klingenberg, Solute carriers involved in energy transfer of
754 mitochondria form a homologous protein family, FEBS Lett. (1987).
755 doi:10.1016/0014-5793(87)81546-6.
756 [33] F. Palmieri, The mitochondrial transporter family (SLC25): Physiological and
757 pathological implications, Pflugers Arch. Eur. J. Physiol. (2004).

758 doi:10.1007/s00424-003-1099-7.
759 [34] F. Palmieri, Diseases caused by defects of mitochondrial carriers: A review,
760 Biochim. Biophys. Acta - Bioenerg. (2008). doi:10.1016/j.bbabio.2008.03.008.
761 [35] E.R.S. Kunji, A.J. Robinson, The conserved substrate binding site of mitochondrial
762 carriers, Biochim. Biophys. Acta - Bioenerg. (2006).
763 doi:10.1016/j.bbabio.2006.03.021.
764 [36] C. Colasante, P. Peña Diaz, C. Clayton, F. Voncken, Mitochondrial carrier family
765 inventory of *Trypanosoma brucei brucei*: Identification, expression and subcellular
766 localisation, Mol. Biochem. Parasitol. 167 (2009) 104–117.
767 doi:10.1016/j.molbiopara.2009.05.004.
768 [37] C. Colasante, V.P. Alibu, S. Kirchberger, J. Tjaden, C. Clayton, F. Voncken,
769 Characterization and developmentally regulated localization of the mitochondrial
770 carrier protein homologue MCP6 from *Trypanosoma brucei*, Eukaryot. Cell. 5
771 (2006). doi:10.1128/EC.00096-06.
772 [38] P. Peña-Diaz, L. Pelosi, C. Ebikeme, C. Colasante, F. Gao, F. Bringaud, F. Voncken,
773 Functional characterization of TbMCP5 , a conserved and essential adp / atp carrier
774 present in the mitochondrion of the human pathogen *Trypanosoma brucei*, J. Biol.
775 Chem. 287 (2012) 41861–41874. doi:10.1074/jbc.M112.404699.
776 [39] C. Colasante, F. Zheng, C. Kemp, F. Voncken, A plant-like mitochondrial carrier
777 family protein facilitates mitochondrial transport of di- and tricarboxylates in
778 *Trypanosoma brucei*, Mol. Biochem. Parasitol. 221 (2018).
779 doi:10.1016/j.molbiopara.2018.03.003.
780 [40] F. Sievers, A. Wilm, D. Dineen, T.J. Gibson, K. Karplus, W. Li, R. Lopez, H.
781 McWilliam, M. Remmert, J. Söding, J.D. Thompson, D.G. Higgins, Fast, scalable
782 generation of high-quality protein multiple sequence alignments using Clustal

783 Omega., Mol. Syst. Biol. 7 (2011) 539. doi:10.1038/msb.2011.75.
784 [41] W. Li, A. Cowley, M. Uludag, T. Gur, H. McWilliam, S. Squizzato, Y.M. Park, N.
785 Buso, R. Lopez, The EMBL-EBI bioinformatics web and programmatic tools
786 framework., Nucleic Acids Res. 43 (2015) W580-4. doi:10.1093/nar/gkv279.
787 [42] S. Kumar, G. Stecher, K. Tamura, MEGA7: Molecular Evolutionary Genetics
788 Analysis Version 7.0 for Bigger Datasets., Mol. Biol. Evol. 33 (2016) 1870–4.
789 doi:10.1093/molbev/msw054.
790 [43] N. Saitou, M. Nei, The neighbor-joining method: a new method for reconstructing
791 phylogenetic trees., Mol. Biol. Evol. 4 (1987) 406–25.
792 [44] S. Biebinger, S. Rettenmaier, J. Flaspohler, C. Hartmann, J. Peña-Diaz, L. Elizabeth
793 Wirtz, H.R. Hotz, J.D. Barry, C. Clayton, The PARP promoter of *Trypanosoma*
794 *brucei* is developmentally regulated in a chromosomal context, Nucleic Acids Res.
795 24 (1996) 1202–1211. doi:10.1093/nar/24.7.1202.
796 [45] E.M. Froschauer, R.J. Schweyen, G. Wiesenberger, The yeast mitochondrial carrier
797 proteins Mrs3p/Mrs4p mediate iron transport across the inner mitochondrial
798 membrane., Biochim. Biophys. Acta. 1788 (2009) 1044–50.
799 doi:10.1016/j.bbamem.2009.03.004.
800 [46] R.D. Gietz, R.A. Woods, Transformation of yeast by lithium acetate/single-stranded
801 carrier DNA/polyethylene glycol method, Methods Enzymol. 350 (2002) 87–96.
802 doi:10.1016/S0076-6879(02)50957-5.
803 [47] E. Garí, L. Piedrafita, M. Aldea, E. Herrero, A set of vectors with a tetracycline-
804 regulatable promoter system for modulated gene expression in Saccharomyces
805 cervisiae, Yeast. (1997). doi:10.1002/(SICI)1097-0061(199707)13:9<837::AID-
806 YEA145>3.0.CO;2-T.
807 [48] F. Voncken, F. Gao, C. Wadforth, M. Harley, C. Colasante, The Phosphoarginine

808 Energy-Buffering System of *Trypanosoma brucei* Involves Multiple Arginine
809 Kinase Isoforms with Different Subcellular Locations, PLoS One. (2013).
810 doi:10.1371/journal.pone.0065908.
811 [49] S. Krieger, W. Schwarz, M.R. Ariyanayagam, A.H. Fairlamb, R.L. Krauth-Siegel, C.
812 Clayton, Trypanosomes lacking trypanothione reductase are avirulent and show
813 increased sensitivity to oxidative stress., Mol. Microbiol. 35 (2000) 542–52.
814 [50] F. Voncken, J.J. Van Hellemond, I. Pfisterer, A. Maier, S. Hillmer, C. Clayton,
815 Depletion of GIM5 causes cellular fragility, a decreased glycosome number, and
816 reduced levels of ether-linked phospholipids in trypanosomes, J. Biol. Chem. 278
817 (2003) 35299–35310. doi:10.1074/jbc.M301811200.
818 [51] V. Bellofatto, J.B. Palenchar, RNA interference as a genetic tool in trypanosomes,
819 Methods Mol. Biol. 442 (2008) 83–94. doi:10.1007/978-1-59745-191-8-7.
820 [52] A. Schneider, D. Bursać, T. Lithgow, The direct route: a simplified pathway for
821 protein import into the mitochondrion of trypanosomes, Trends Cell Biol. 18 (2008)
822 12–18. doi:10.1016/j.tcb.2007.09.009.
823 [53] J. Riemer, H. Hoepken, H. Czerwinska, S.R. Robinson, R. Dringen, Colorimetric
824 ferrozine-based assay for the quantitation of iron in cultured cells, 331 (2004) 370–
825 375. doi:10.1016/j.ab.2004.03.049.
826 [54] F.Y. Li, B. Leibiger, I. Leibiger, C. Larsson, Characterization of a putative murine
827 mitochondrial transporter homology of hMRS3/4, Mamm. Genome. (2002).
828 doi:10.1007/s00335-001-2094-y.
829 [55] F. Palmieri, The mitochondrial transporter family (SLC25): Physiological and
830 pathological implications, Pflugers Arch. Eur. J. Physiol. 447 (2004) 689–709.
831 doi:10.1007/s00424-003-1099-7.
832 [56] H. Aquila, D. Misra, M. Eulitz, M. Klingenberg, Complete amino acid sequence of

833 the ADP/ATP carrier from beef heart mitochondria., Hoppe-Seyler's Zeitschrift Für
834 Physiol. Chemie. 363 (1982) 345–9. http://www.ncbi.nlm.nih.gov/pubmed/7076130.
835 [57] M. Saraste, J.E. Walker, Internal sequence repeats and the path of polypeptide in
836 mitochondrial ADP/ATP translocase, FEBS Lett. 144 (1982) 250–254.
837 doi:10.1016/0014-5793(82)80648-0.
838 [58] A.J. Robinson, E.R.S. Kunji, Mitochondrial carriers in the cytoplasmic state have a
839 common substrate binding site, Proc. Natl. Acad. Sci. (2006).
840 doi:10.1073/pnas.0509994103.
841 [59] M. Gutiérrez-Aguilar, C.P. Baines, Physiological and pathological roles of
842 mitochondrial SLC25 carriers, Biochem. J. (2013). doi:10.1042/BJ20121753.
843 [60] V. Zara, A. Ferramosca, P. Robitaille-Foucher, F. Palmieri, J.C. Young,
844 Mitochondrial carrier protein biogenesis: Role of the chaperones Hsc70 and Hsp90,
845 Biochem. J. (2009). doi:10.1042/BJ20082270.
846 [61] A. Ferramosca, V. Zara, Biogenesis of mitochondrial carrier proteins: Molecular
847 mechanisms of import into mitochondria, Biochim. Biophys. Acta - Mol. Cell Res.
848 (2013). doi:10.1016/j.bbamcr.2012.11.014.
849 [62] B. Stijlemans, A. Beschin, S. Magez, J.A. Van Ginderachter, P. De Baetselier, Iron
850 homeostasis and trypanosoma brucei associated immunopathogenicity development:
851 A battle/quest for iron, Biomed Res. Int. (2015). doi:10.1155/2015/819389.
852 [63] L. Kořený, M. Oborník, J. Lukeš, Make It, Take It, or Leave It: Heme Metabolism of
853 Parasites, PLoS Pathog. (2013). doi:10.1371/journal.ppat.1003088.
854 [64] K.E.J. Tripodi, S.M. Menendez Bravo, J.A. Cricco, Role of heme and heme-proteins
855 in trypanosomatid essential metabolic pathways, Enzyme Res. (2011).
856 [65] V. Hannaert, E. Saavedra, F. Duffieux, J.-P. Szikora, D.J. Rigden, P.A.M. Michels,
857 F.R. Opperdoes, Plant-like traits associated with metabolism of Trypanosoma

858 parasites., Proc. Natl. Acad. Sci. U. S. A. 100 (2003) 1067–71.
859 doi:10.1073/pnas.0335769100.
860 [66] P.J. Keeling, Diversity and evolutionary history of plastids and their hosts, Am. J.
861 Bot. 91 (2004) 1481–1493. doi:10.3732/ajb.91.10.1481.
862 [67] P.J. Keeling, J.D. Palmer, Horizontal gene transfer in eukaryotic evolution, Nat. Rev.
863 Genet. 9 (2008) 605–618. doi:10.1038/nrg2386.
864 [68] F.R. Opperdoes, P.A.M. Michels, Horizontal gene transfer in trypanosomatids.,
865 Trends Parasitol. 23 (2007) 470–476. doi:10.1016/j.pt.2007.08.002.
866 [69] M.D. Fleming, D.R. Campagna, J.N. Haslett, C.C. Trenor, N.C. Andrews, A
867 mutation in a mitochondrial transmembrane protein is responsible for the pleiotropic
868 hematological and skeletal phenotype of flexed-tail (f/f) mice, Genes Dev. 15 (2001)
869 652–657. doi:10.1101/gad.873001.
870 [70] X. Ye, J. Xu, C. Cheng, G. Yin, L. Zeng, C. Ji, S. Gu, Y. Xie, Y. Mao, Isolation and
871 characterization of a novel human putative anemia-related gene homologous to
872 mouse sideroflexin, Biochem. Genet. (2003). doi:10.1023/A:1022026001114.
873 [71] D.R. Richardson, D.J.R. Lane, E.M. Becker, M.L.H. Huang, M. Whitnall, Y.S.
874 Rahmanto, A.D. Sheftel, P. Ponka, Mitochondrial iron trafficking and the integration
875 of iron metabolism between the mitochondrion and cytosol, Proc. Natl. Acad. Sci. U.
876 S. A. (2010). doi:10.1073/pnas.0912925107.
877 [72] P.N. Paradkar, K.B. Zumbrennen, B.H. Paw, D.M. Ward, J. Kaplan, Regulation of
878 mitochondrial iron import through differential turnover of mitoferrin 1 and
879 mitoferrin 2, Mol. Cell. Biol. (2009). doi:10.1128/mcb.01685-08.
880 [73] L. Li, J. Kaplan, A mitochondrial-vacuolar signaling pathway in yeast that affects
881 iron and copper metabolism, J. Biol. Chem. 279 (2004) 33653–33661.
882 doi:10.1074/jbc.M403146200.

883 [74] K. Bashir, Y. Ishimaru, H. Shimo, S. Nagasaka, M. Fujimoto, H. Takanashi, N.
884 Tsutsumi, G. An, H. Nakanishi, N.K. Nishizawa, The rice mitochondrial iron
885 transporter is essential for plant growth, Nat. Commun. 2 (2011) 322–327.
886 doi:10.1038/ncomms1326.
887 [75] B. Stijlemans, A. Vankrunkelsven, L. Brys, S. Magez, P. De Baetselier, Role of iron
888 homeostasis in trypanosomiasis-associated anemia, Immunobiology. (2008).
889 doi:10.1016/j.imbio.2008.07.023.
890 [76] D. Steverding, Bloodstream forms of *Trypanosoma brucei* require only small
891 amounts of iron for growth, Parasitol. Res. (1997). doi:10.1007/s004360050357.
892 [77] H.G.A.M. Van Luenen, R. Kieft, R. Mußmann, M. Engstler, B. Ter Riet, P. Borst,
893 Trypanosomes change their transferrin receptor expression to allow effective uptake
894 of host transferrin, Mol. Microbiol. (2005). doi:10.1111/j.1365-2958.2005.04831.x.
895
896 **AKNOWLEDGEMENT**
897 We thank Christine Clayton for proof-reading the manuscript.
898 This work was funded by the BBSRC, grant number BB/G00448X/1.
899
900 **CONFLICT OF INTEREST**
901 The authors declare that they have no conflicts of interest with the contents of this article.
902
903 **AUTHOR CONTRIBUTION**
904 FZ, CC and FV designed all the experiments presented in this paper and experiments were
905 conducted by FZ. All authors reviewed the results and contributed equally to the drafting and
906 correction of the manuscript as well as to the design of the figures. The final version of the
907 manuscript was approved by all authors.